

Figure S1. Aqueous KCl solution conductivity as function of reciprocal of resistance.

Table S1. Resistance and conductivity of 1 mol dm<sup>-3</sup> NaClO<sub>4</sub> in 1:1 EC/DEC electrolyte at various temperatures

Temperature (°C)	Resistance ( $\Omega$ )	Conductivity ( $S m^{-1}$ )
10	561	0.566
15	501	0.633
20	468	0.678
25	396	0.802
40	370	0.857
50	318	0.999
60	271	1.17
70	236	1.34
80	220	1.44

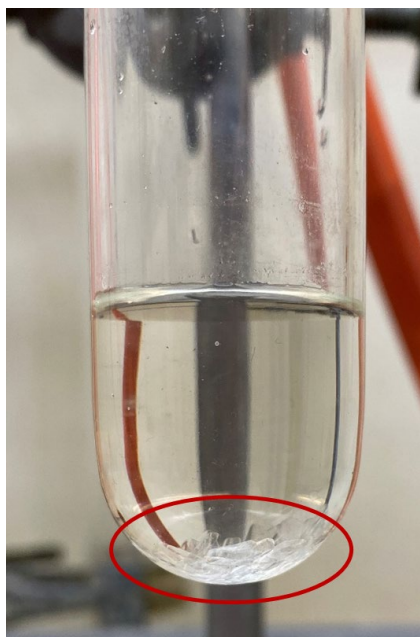


Figure S2. Photograph of  $1 \text{ mol dm}^{-3} \text{ NaClO}_4$  in 1:1 EC/DEC after standing overnight around  $20^\circ \text{C}$ .

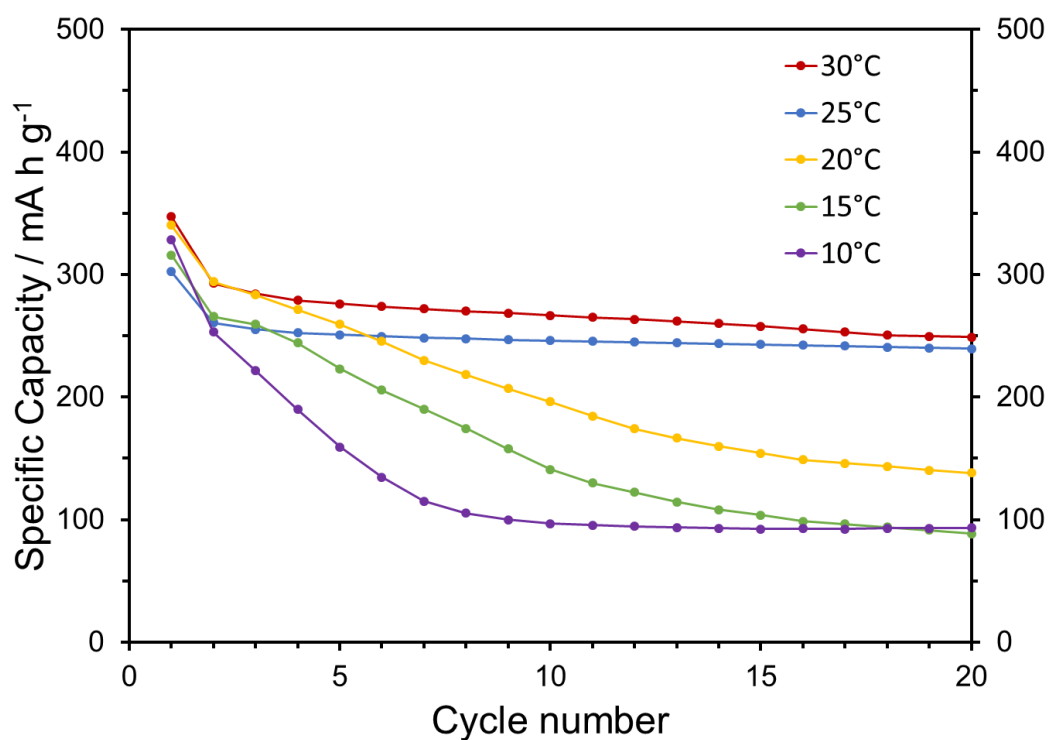


Figure S3. Reduction specific capacity of HC at temperatures from 10 to  $30^\circ \text{C}$  between 0.001 and 2 V (vs.  $\text{Na}^+/\text{Na}$ ) at  $100 \text{ mA g}^{-1}$  in sodium half-cells.

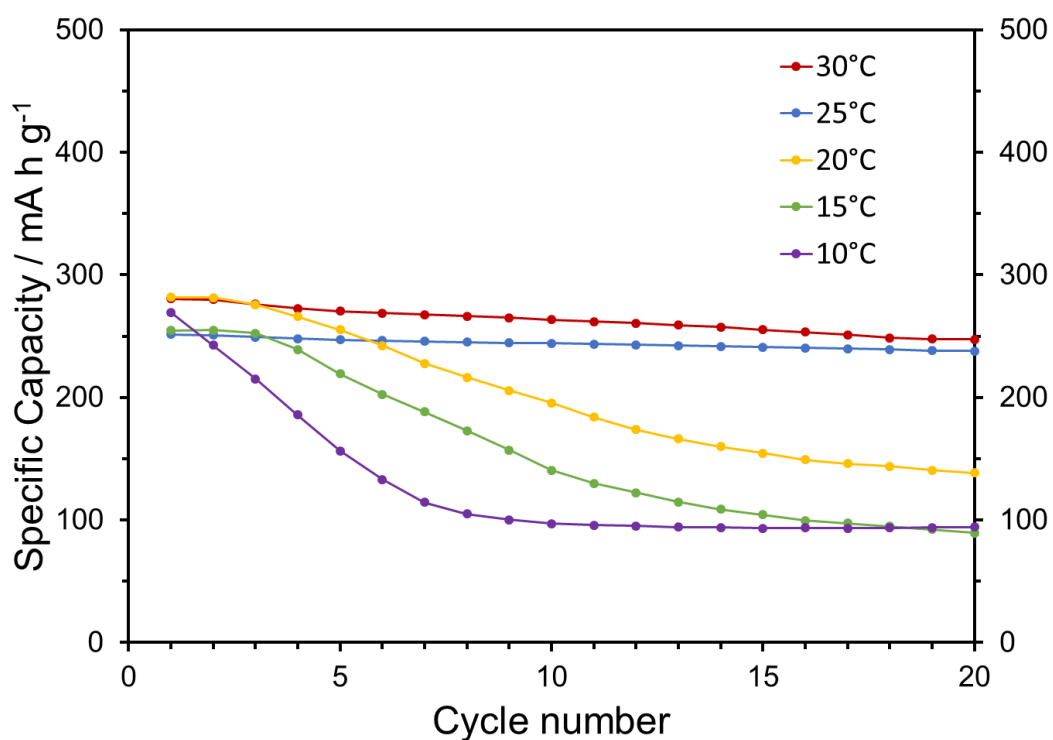


Figure S4. Oxidation specific capacity of HC at temperatures from 10 to 30 °C between 0.001 and 2 V (vs. Na<sup>+</sup>/Na) at 100 mA g<sup>-1</sup> in sodium half-cells.

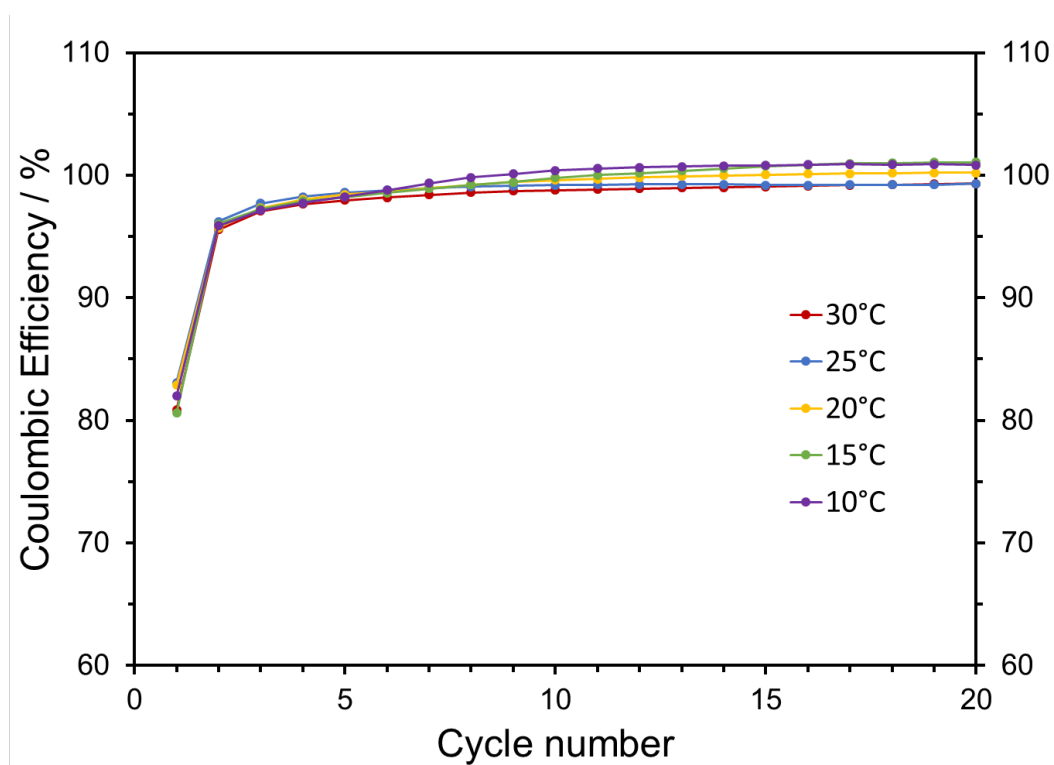


Figure S5. Coulombic efficiency of HC at temperatures from 10 to 30 °C cycled between 0.001 and 2 V (vs. Na<sup>+</sup>/Na) at 100 mA g<sup>-1</sup> in sodium half-cells.

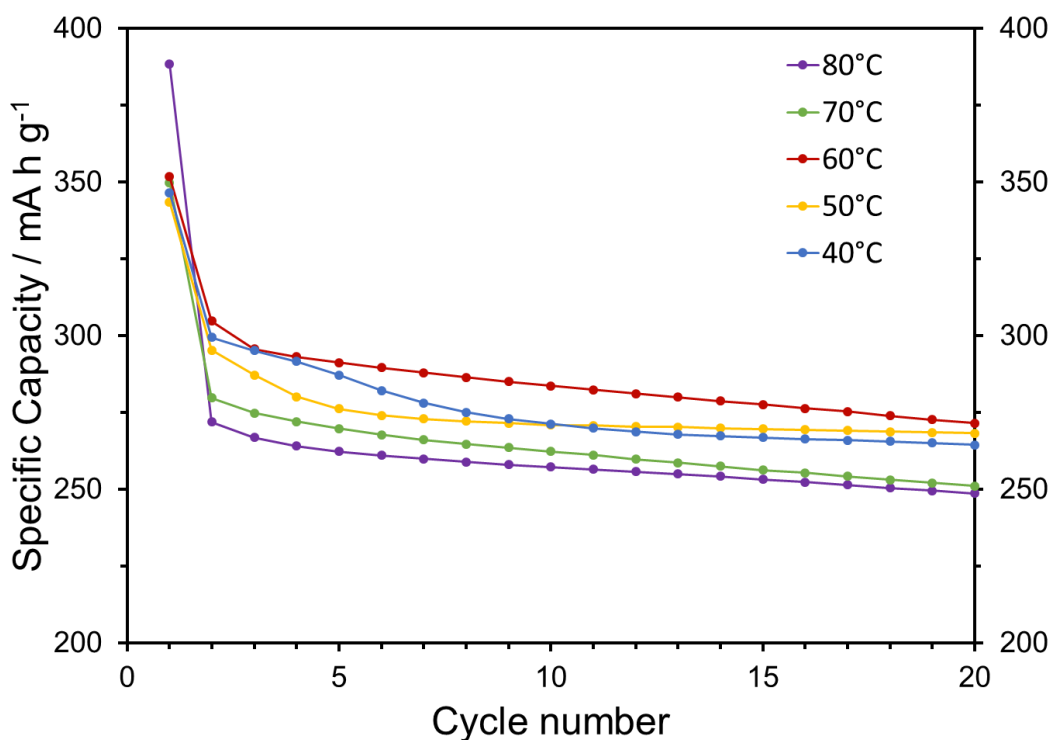


Figure S6. Reduction specific capacity of HC at temperatures from 40 to 80 °C between 0.001 and 2 V (vs. Na<sup>+</sup>/Na) at 100 mA g<sup>-1</sup> in sodium half-cells.

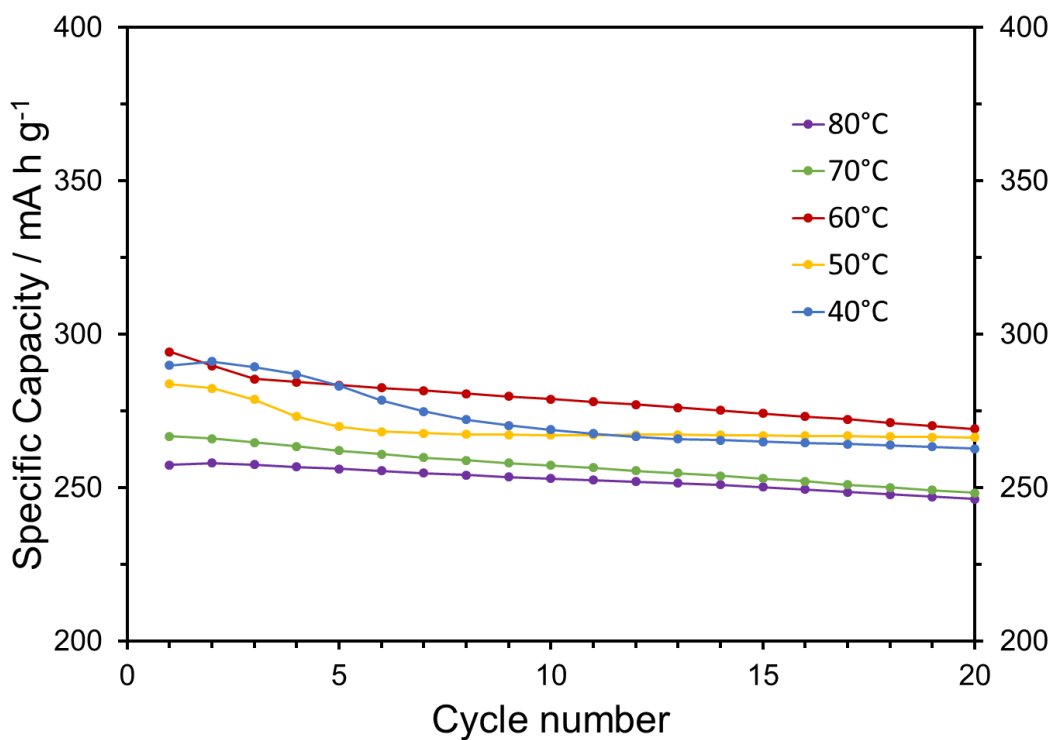


Figure S7. Oxidation specific capacity of HC at temperatures from 40 to 80 °C between 0.001 and 2 V (vs. Na<sup>+</sup>/Na) at 100 mA g<sup>-1</sup> in sodium half-cells.

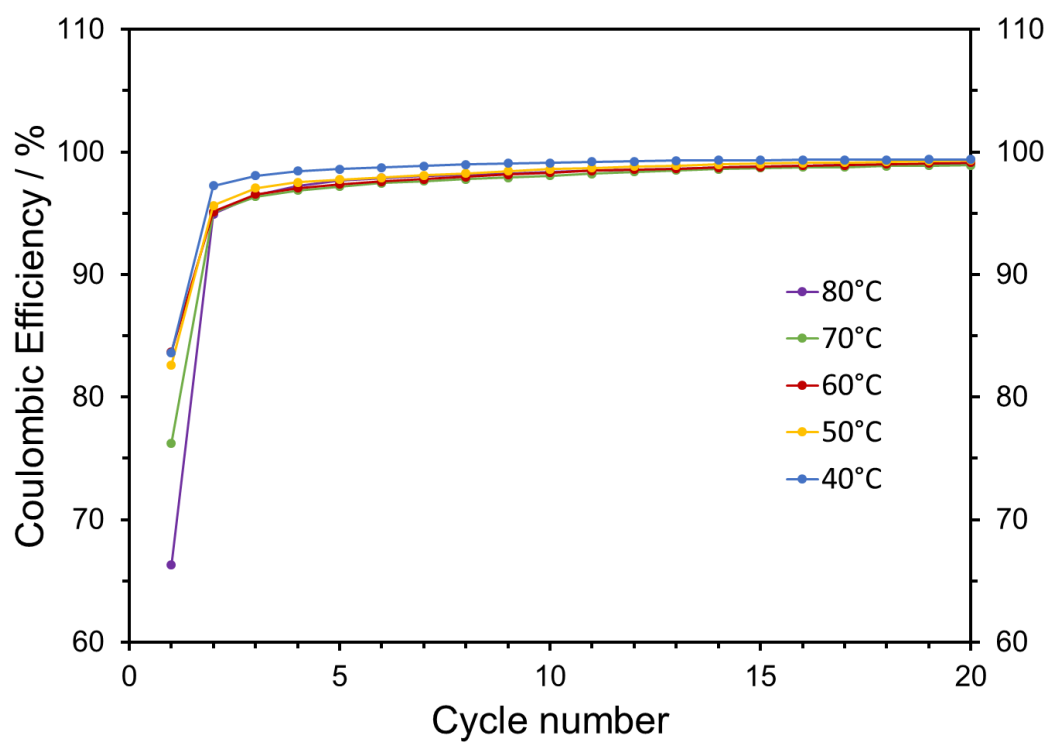


Figure S8. Coulombic efficiency of HC at temperatures from 40 to 80 °C cycled between 0.001 and 2 V (vs. Na<sup>+</sup>/Na) at 100 mA g<sup>-1</sup> in sodium half-cells.

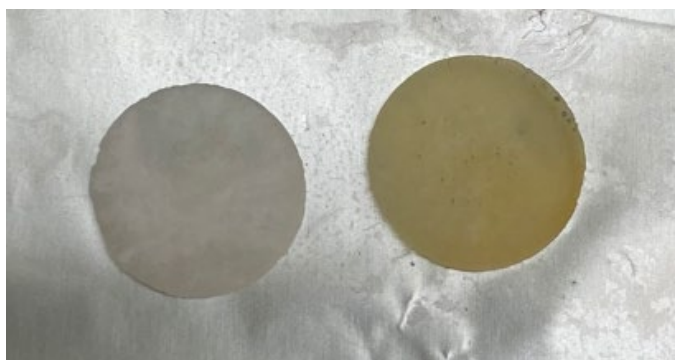


Figure S9. Separators (12 mm discs) after 20 cycles at 25 °C (left) and 60 °C (right).

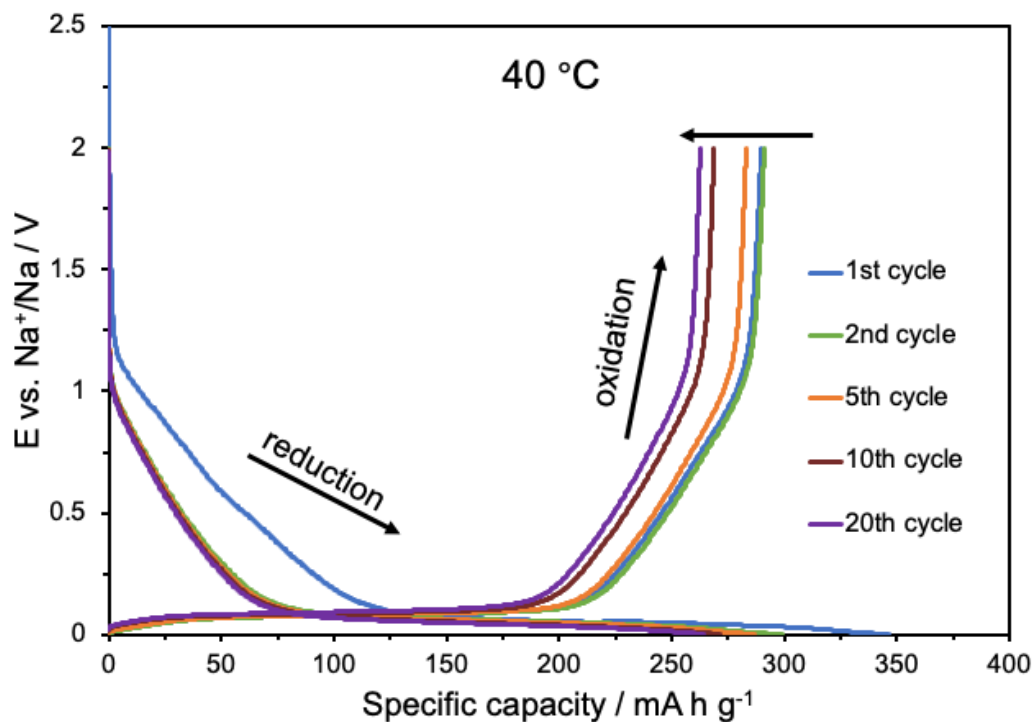


Figure S10. Voltage-capacity plots of galvanostatic cycling data at  $100 \text{ mA g}^{-1}$  current for HC at the 1<sup>st</sup>, 2<sup>nd</sup>, 5<sup>th</sup>, 10<sup>th</sup> and 20<sup>th</sup> cycle at 40 °C.

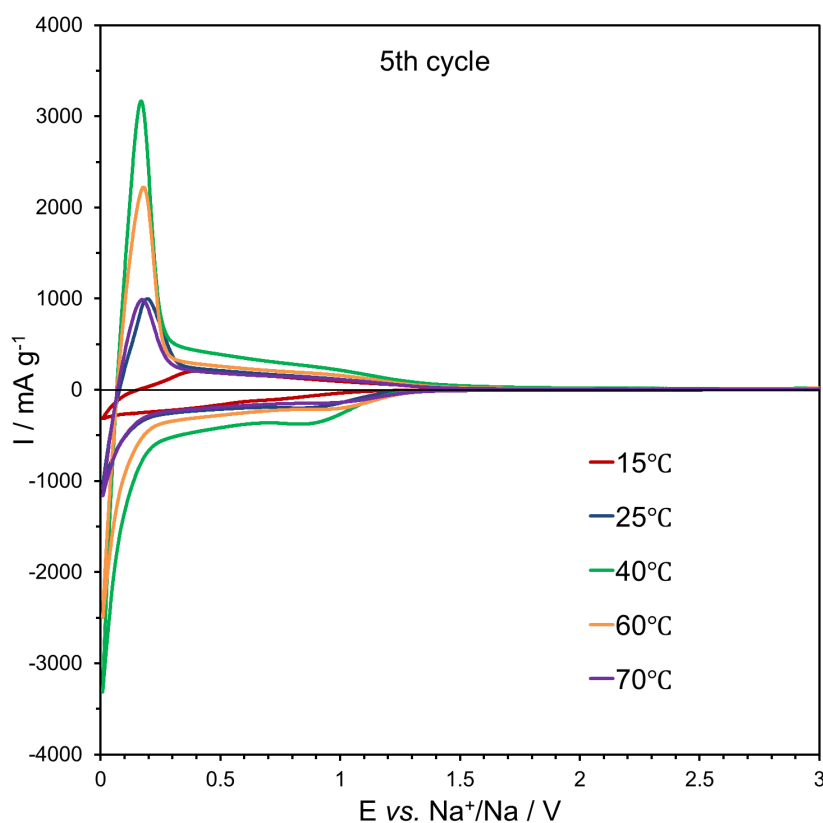


Figure S11. CV profile of the 5<sup>th</sup> cycle of HC at temperatures from 15 to 70 °C at  $1 \text{ mV s}^{-1}$  scan rate between 3 and 0.01 V vs.  $\text{Na}^+/\text{Na}$ .

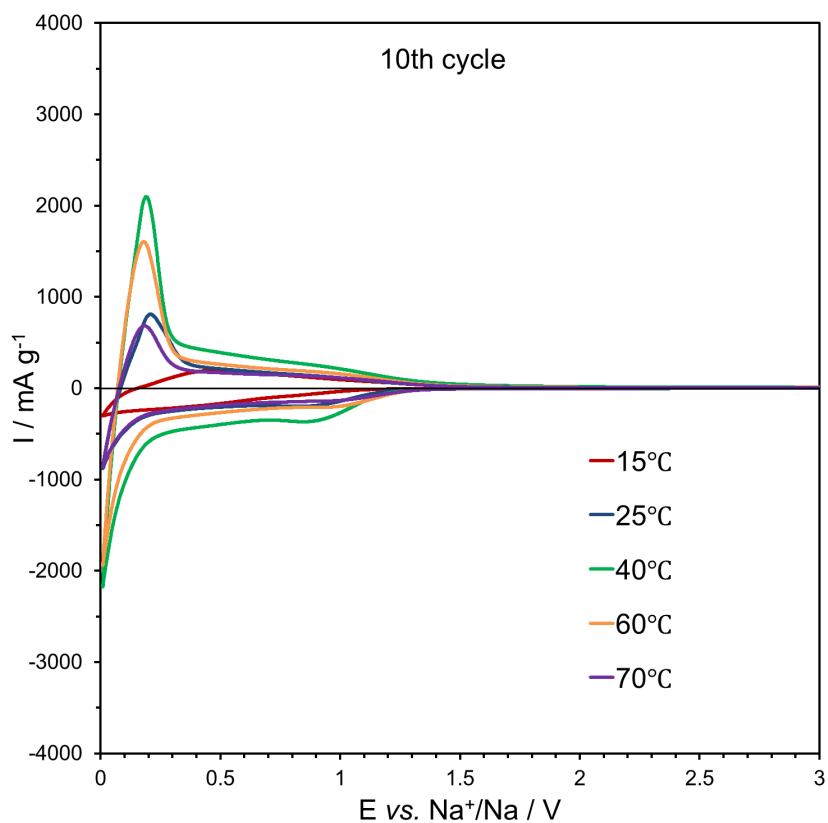


Figure S12. CV profile of the 10<sup>th</sup> cycle of HC at temperatures from 15 to 70 °C at 1 mV s<sup>-1</sup> scan rate between 3 and 0.01 V vs. Na<sup>+</sup>/Na.

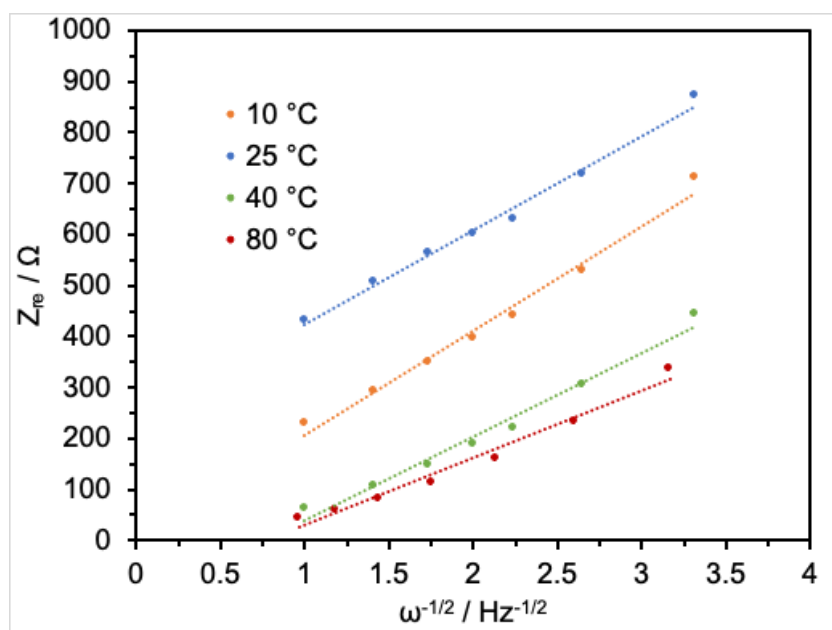


Figure S13. The relationship between  $Z_{re}$  and  $\omega^{-1/2}$  at low frequency with freshly prepared cells at 10, 25, 40 and 80 °C

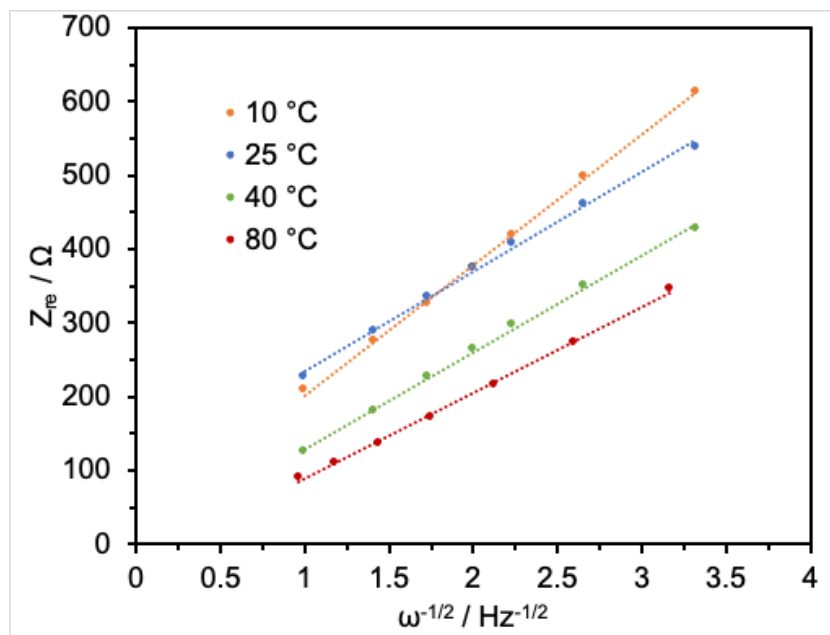


Figure S14. The relationship between  $Z_{re}$  and  $\omega^{-1/2}$  at low frequency with cycled 19 times cells at 10, 25, 40 and 80 °C.

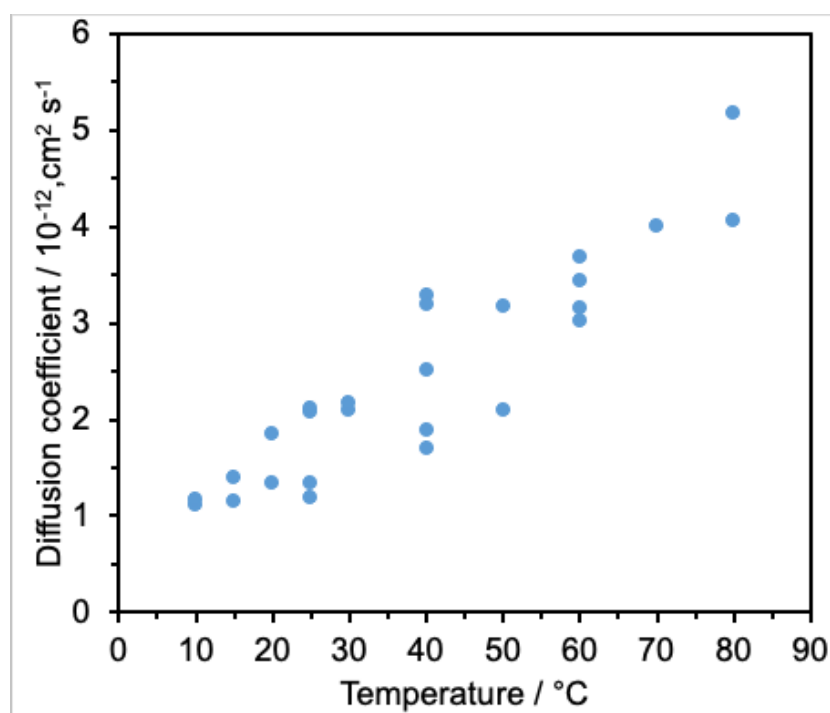


Figure S15. Na ion diffusion coefficients after 19 cycles at temperatures from 10 to 80 °C.

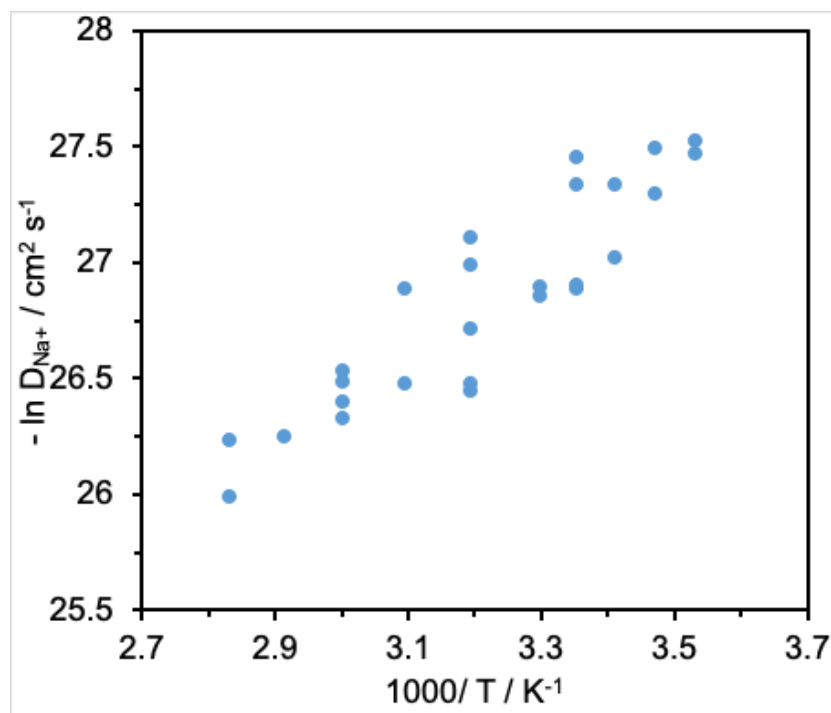


Figure S16. Dependence of the natural logarithm of the Na<sup>+</sup> diffusion coefficient on reciprocal temperature.

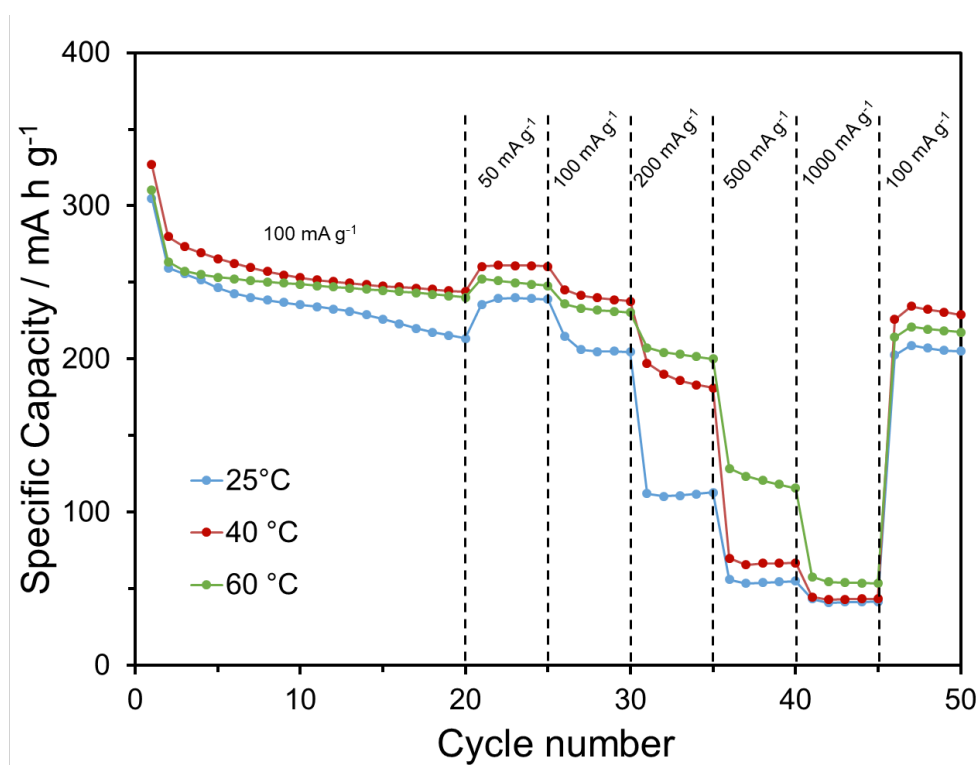


Figure S17. Rate capability of HC reduction capacity at different current densities and at temperatures of 25, 40 and 60 °C.

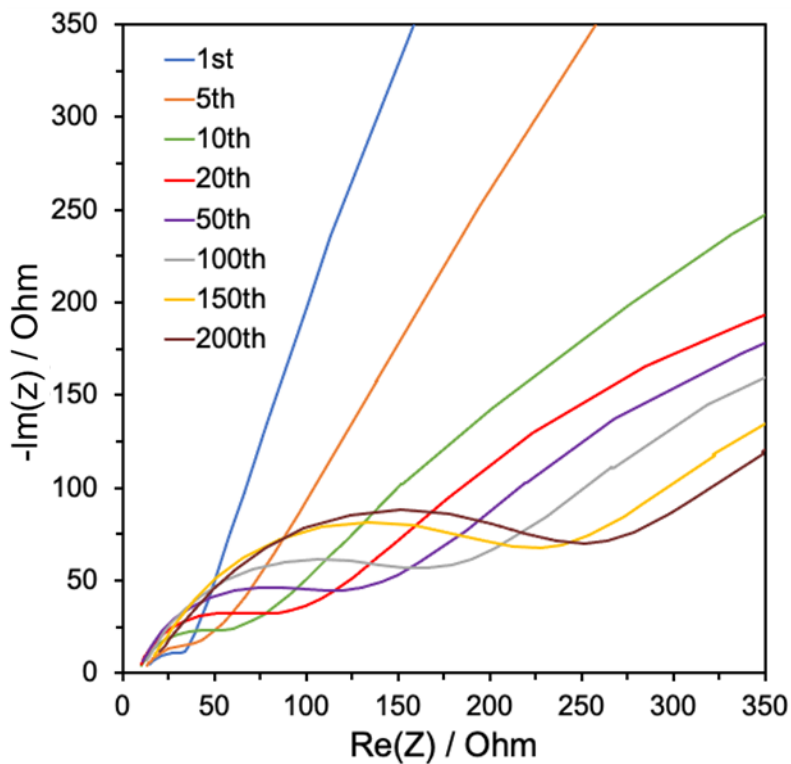


Figure S18. Nyquist plots of HC electrode after different numbers of cycles at 25 °C long-term cycling.

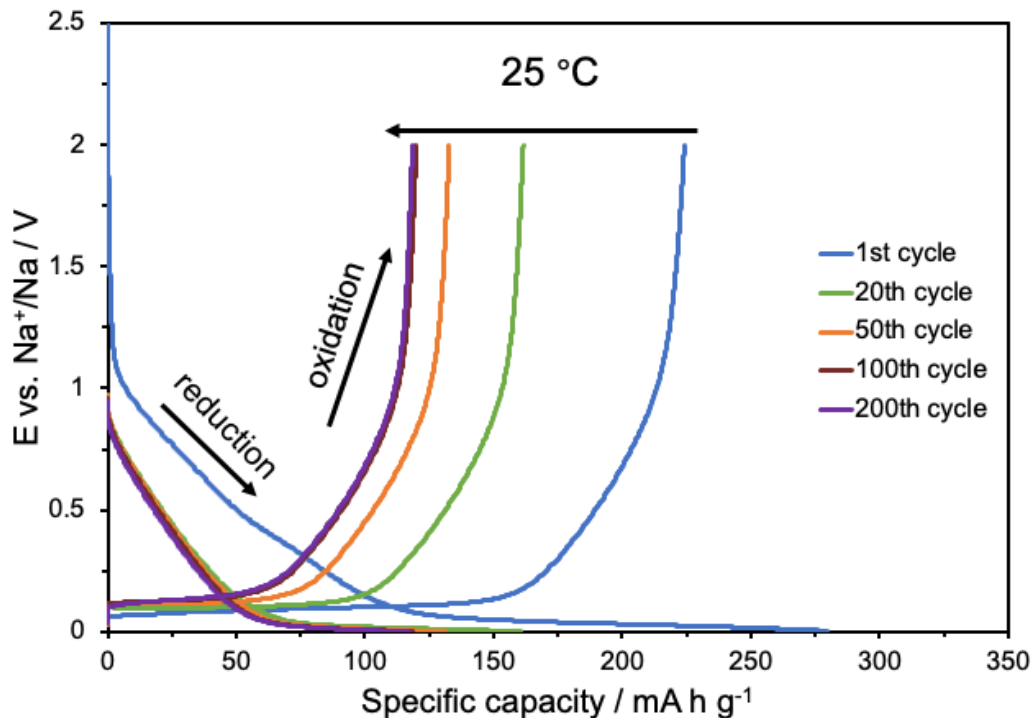


Figure S19. Voltage-capacity plots of galvanostatic cycling data at 100 mA g<sup>-1</sup> current for HC at the 1<sup>st</sup>, 20<sup>th</sup>, 50<sup>th</sup>, 100<sup>th</sup> and 200<sup>th</sup> cycle at 25 °C.

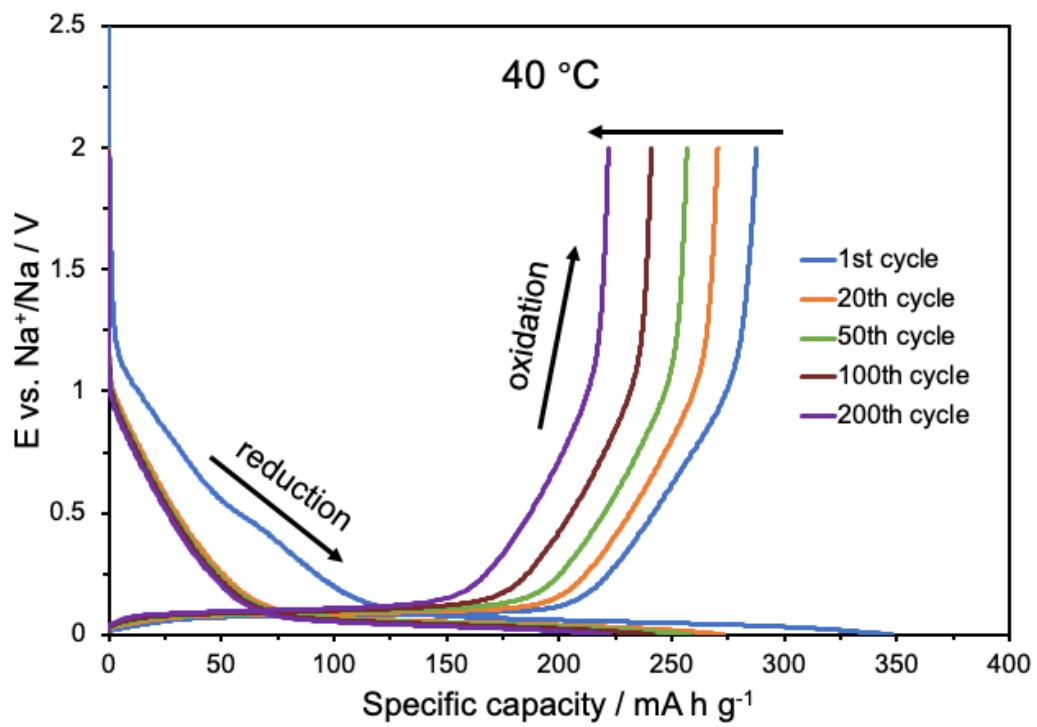


Figure S20. Voltage-capacity plots of galvanostatic cycling data at 100 mA g<sup>-1</sup> current for HC at the 1<sup>st</sup>, 20<sup>th</sup>, 50<sup>th</sup>, 100<sup>th</sup> and 200<sup>th</sup> cycle at 40 °C.